

# Induction of Broad Cytotoxic T Cells by Protective DNA Vaccination Against Marburg and Ebola

Devon J Shedlock<sup>1</sup>, Jenna Aviles<sup>2</sup>, Kendra T Talbott<sup>1</sup>, Gary Wong<sup>2</sup>, Stephan J Wu<sup>1</sup>, Daniel O Villarreal<sup>1</sup>, Devin JF Myles<sup>1</sup>, Maria A Croyle<sup>3</sup>, Jian Yan<sup>4</sup>, Gary P Kobinger<sup>2,5,6</sup> and David B Weiner<sup>1</sup>

<sup>1</sup>Department of Pathology & Laboratory Medicine, Perelman School of Medicine, University of Pennsylvania, Philadelphia, Pennsylvania, USA; <sup>2</sup>Department of Medical Microbiology, University of Manitoba, Winnipeg, Manitoba, Canada; <sup>3</sup>Division of Pharmaceutics, College of Pharmacy, and Institute of Cellular and Molecular Biology, The University of Texas at Austin, Austin, Texas, USA; <sup>4</sup>R&D Department, Inovio Pharmaceuticals Inc., Blue Bell, Pennsylvania, USA; <sup>5</sup>Special Pathogens Program, National Microbiology Laboratory, Public Health Agency of Canada, Winnipeg, Manitoba, Canada; <sup>6</sup>Department of Immunology, University of Manitoba, Winnipeg, Manitoba, Canada

Marburg and Ebola hemorrhagic fevers have been described as the most virulent viral diseases known to man due to associative lethality rates of up to 90%. Death can occur within days to weeks of exposure and there is currently no licensed vaccine or therapeutic. Recent evidence suggests an important role for antiviral T cells in conferring protection, but little detailed analysis of this response as driven by a protective vaccine has been reported. We developed a synthetic polyvalent-filovirus DNA vaccine against *Marburg marburgvirus* (MARV), *Zaire ebolavirus* (ZEBOV), and *Sudan ebolavirus* (SUDV). Preclinical efficacy studies were performed in guinea pigs and mice using rodent-adapted viruses, whereas murine T-cell responses were extensively analyzed using a novel modified assay described herein. Vaccination was highly potent, elicited robust neutralizing antibodies, and completely protected against MARV and ZEBOV challenge. Comprehensive T-cell analysis revealed cytotoxic T lymphocytes (CTLs) of great magnitude, epitopic breadth, and T<sub>H</sub>1-type marker expression. This model provides an important preclinical tool for studying protective immune correlates that could be applied to existing platforms. Data herein support further evaluation of this enhanced gene-based approach in nonhuman primate studies for in depth analyses of T-cell epitopes in understanding protective efficacy.

Received 29 November 2012; accepted 12 February 2013; advance online publication 14 May 2013. doi:10.1038/mt.2013.61

## INTRODUCTION

Marburg and Ebola viruses cause severe hemorrhagic fever disease in humans with associative lethality rates of up to 90%.<sup>1</sup> Capable of causing death within days to weeks of exposure, they have been described as “one of the most virulent viral diseases known to man” and there is no licensed vaccine or therapeutic available. Despite unpredictable endemic surfacing primarily in central Africa, including recent outbreaks in Uganda and Democratic Republic of the Congo (DRC), they typically occur in resource-limited settings and pose little risk to public health

worldwide.<sup>2</sup> However, filoviruses remain a concern due to their high lethality rates, the lack of effective countermeasures, and the threat they pose to national security if weaponized. The US Centers for Disease Control and Prevention has classified them as “Category A Bioterrorism Agents” as they, in theory, could be easily transmitted, result in high mortality, cause major public health impact and panic, and require special action for public health preparedness (<http://www.bt.cdc.gov/agent/agentlist-category.asp#catdef>).<sup>3</sup> An effective vaccine could be incorporated into national biodefense stockpiles while also benefitting individuals against potential exposure in the laboratory or through ecological work, as well as medical and public health personnel involved in hands-on outbreak response activities.<sup>2</sup>

Countermeasure development will ultimately require an improved understanding of protective immune correlates and how they are modulated during infection. This proves difficult when infected individuals who succumb to filoviral disease fail to mount an early immune response.<sup>4</sup> These fast-moving hemorrhagic fever diseases result in immune dysregulation, as demonstrated by the lack of a virus-specific Ab response and a great reduction in gross T-cell numbers,<sup>5</sup> leading to uncontrolled viral replication and multi-organ infection and failure. Conversely, survivors of Ebola virus (EBOV) disease exhibit an early and transient IgM response, which is quickly followed by increasing levels of virus-specific IgG and cytotoxic T lymphocytes (CTL).<sup>4,5</sup> These observations suggest that humoral and cell-mediated immune responses play a role in conferring protection against disease.<sup>4,6,7</sup> These data are also supported by numerous preclinical efficacy studies demonstrating the contribution of vaccine-induced adaptive immunity to the protection against lethal challenge (**Supplementary Note S1**).<sup>8</sup> However, mounting evidence has demonstrated a critical role for T cells in providing protection<sup>7,9–11</sup> where efficacy was greatly associated with the functional phenotype of CD8<sup>+</sup> T cells.<sup>4,12</sup> Although these recent studies highlight the importance of T cells in providing protection, their precise contributions remain uncharacterized and controversial. Furthermore, little detailed analysis of this response driven by a protective vaccine has been reported.

To help expand upon these data, we developed a novel polyvalent-filovirus vaccine comprised by three DNA plasmids

Correspondence: David B Weiner, Department of Pathology & Laboratory Medicine, Perelman School of Medicine, University of Pennsylvania, 422 Curie Blvd, 505 Stellar-Chance Laboratories, Philadelphia, Pennsylvania, USA. E-mail: [dbweiner@mail.med.upenn.edu](mailto:dbweiner@mail.med.upenn.edu)

encoding the envelope glycoprotein (GP) genes of *Marburg marburgvirus* (MARV), *Sudan ebolavirus* (SUDV), or *Zaire ebolavirus* (ZEBOV), adopting the multiagent approach (**Supplementary Note S2**),<sup>13–17</sup> and determined its capacity for inducing protective efficacy and broad CTL in rodent preclinical studies. In addition, T-cell responses were extensively analyzed including the use of a novel method for epitope identification and characterization described herein. As a filoviral vaccine candidate, an “enhanced” DNA (E-DNA)-based platform exhibits many advantages given recent advances in genetic optimization and delivery techniques (**Supplementary Note S3**).<sup>18–20</sup> As such, each GP was genetically optimized, subcloned into modified mammalian expression vectors, and then delivered using *in vivo* electroporation.<sup>19</sup> Vaccination in preclinical rodent studies induced robust neutralizing Abs (NABs) and CTL expressing T<sub>h</sub>1-type markers, and was completely protective against challenge with MARV and ZEBOV. Furthermore, vaccine-induced T-cell responses exhibited great epitopic breadth as extensively analyzed using a novel modified

assay described herein.<sup>21</sup> In total, 52 novel T-cell epitopes from two different mouse genetic backgrounds were identified (19 of 20 MARV epitopes, 15 of 16 SUDV, and 18 of 22 ZEBOV) and occurred primarily in highly conserved regions of their respective GPs. These data represent the most comprehensive report of pre-clinical GP epitopes to date, and provides a tool by which T-cell responses may be further evaluated in comparative studies and in relation to protective efficacy in the preclinic, and later in nonhuman primate studies.

## RESULTS

### Vaccine construction and expression

Phylogenetic analysis revealed relative conservation among the EBOV GPs (94.4% for SUDV and 92.9% for ZEBOV), whereas the MARV GP (MGP) were more divergent (~70% conserved) (**Figure 1a**). Thus, a consensus strategy, as determined by alignment of the prevailing ZEBOV and SUDV GP amino acid sequences, was adopted for the EBOV GPs, whereas a type-matched strategy

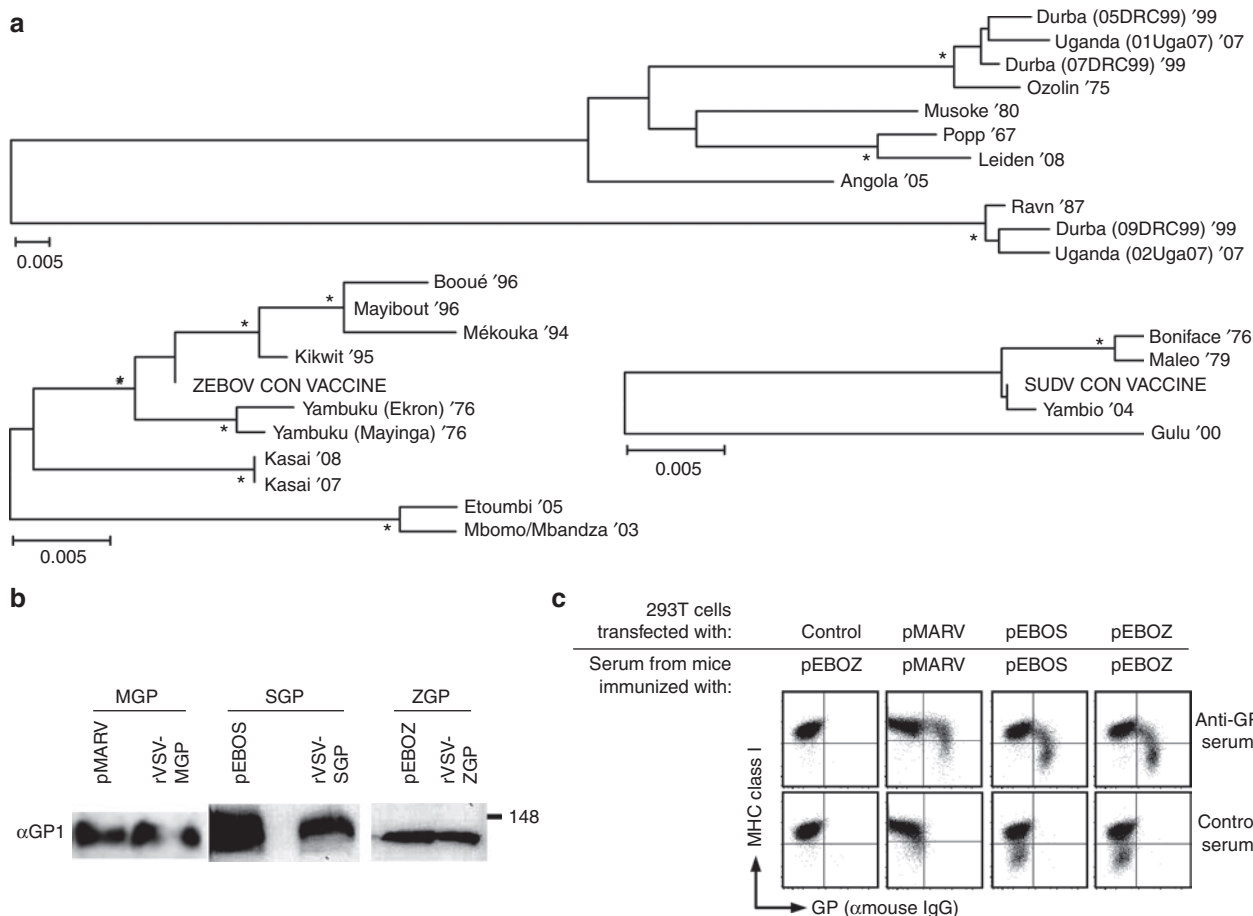


**Figure 1** Polyvalent-vaccine construction and expression. **(a)** Phylogenetic trees for MGP (top), SGP (lower right), and ZGP (lower left) are shown. \*Significant support values as verified by bootstrap analysis. A consensus strategy was adopted for the ZGP and SGP immunogens (CON VACCINE). Scale bars signify distance of amino acids per site and analyses were conducted using *MEGA* version 5 software. GP transgenes were commercially synthesized, genetically optimized, and subcloned into modified pVAX1 mammalian expression vectors. Ag expression was analyzed following transfection of HEK 293T cells by **(b)** western immunoblotting and **(c)** FACS. For a comparative control, rVSV expressing MGP, SGP, or ZGP was run concurrently with each GP sample and species-specific anti-GP1 mAbs were used for detection. Size is indicated (kDa). For FACS, transfected cells were indirectly stained with mouse-derived GP-specific serum reagents followed by extensive washing and goat antimouse IgG and MHC class I. Experiments in **b** and **c** were repeated at least three times with similar results. Significance for unrooted phylogenetic trees was determined by maximum-likelihood method and verified by bootstrap analysis and significant support values ( $\geq 80\%$ ; 1,000 bootstrap replicates) were determined by *MEGA* version 5 software. rVSV, recombinant vesicular stomatitis viruses; GP, glycoprotein.

was used for MARV using the 2005 Angola outbreak sequence which was solely responsible for the largest and deadliest MARV outbreak.<sup>22</sup> Each GP transgene was genetically optimized, synthesized commercially, and then subcloned into a modified pVAX1 mammalian expression vector. Altogether, a three-plasmid strategy formed the foundation for our novel polyvalent-filovirus vaccine strategy.

HEK 293T cells were transfected separately with each plasmid and GP expression was assessed by western immunoblotting and fluorescence-activated cell sorting (FACS). A ~130 kDa protein was observed for each in cell lysates harvested 48 hours after transfection using species-specific anti-GP1 mAbs for detection (Figure 1b). For a comparative control, recombinant vesicular stomatitis viruses expressing the respective GPs were loaded in concurrent lanes. Next, GP expression on the cell surface was analyzed 24 hours

after transfection by indirect staining with GP-specific or control polyclonal serum by FACS (Figure 1c). Cell surface expression was detected for all vaccine plasmids although little non-specific binding was observed; control serum did not react with GP-transfected cells nor did the positive sera with pVAX1-transfected cells (data shown for pEBOZ). As expected for the EBOV GPs, cell surface expression sterically occluded recognition of surface MHC class I, as well as  $\beta$ 1-integrin (data not shown).<sup>23</sup>

### Complete protection against MARV and ZEBOV challenge

To determine protective efficacy, we used the guinea pig preclinical challenge model (Supplementary Note S4). Guinea pigs ( $n = 24$ ) were immunized with 200  $\mu$ g of each plasmid into three separate vaccination sites or with pVAX1 empty vector control ( $n = 9$ ),

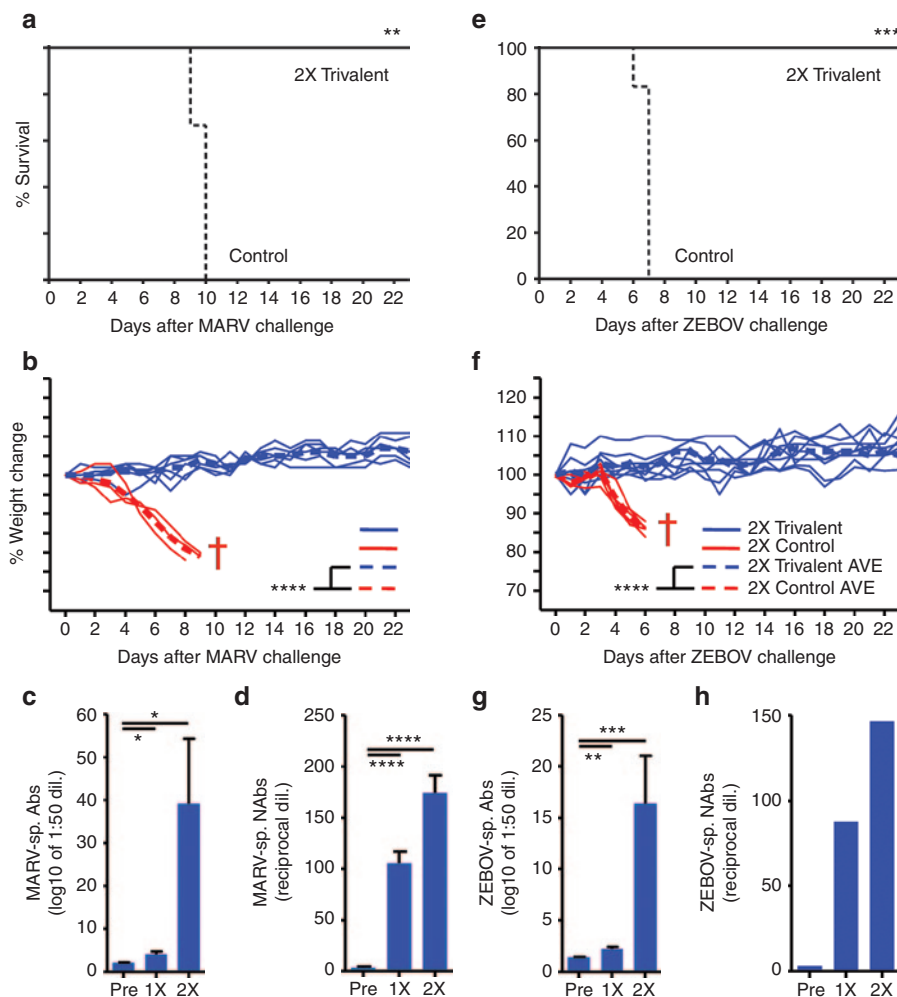


**Figure 2** Complete protection against MARV and ZEBOV challenge. Guinea pigs ( $n = 24$ ) were immunized i.d. two times with 200  $\mu$ g of each of the three E-DNA plasmids at separate vaccination sites. After 28 days, animals were challenged with 1,000 LD<sub>50</sub> of either gpMARV ( $n = 9$ ; left) or gpZEBOV ( $n = 15$ ; right) and then weighed daily and monitored for disease progression. (a,e) Animal survival data and (b,f) % change in body weight are displayed for vaccinated (solid black or blue lines, respectively) and control animals (dashed or solid red lines, respectively;  $n = 3$  for gpMARV and  $n = 6$  for gpZEBOV). Average body weight is displayed as dashed lines (b,f) and daggers (†) denote animals that succumbed to disease. Binding (c,g) Abs and (d,h) NAbs were measured in serum from vaccinated animals before (Pre) and after the first (1X) and second (2X) immunizations. (h) Analysis was conducted on pooled serum. \* $P < 0.1$ ; \*\* $P < 0.01$ ; \*\*\* $P < 0.001$ ; \*\*\*\* $P < 0.0001$ . Experiments were performed in a BSL-4 facility and repeated twice with similar results and error bars represent SEM. Group analyses were completed by matched, two-tailed, unpaired  $t$ -test and survival curves were analyzed by log-rank (Mantel-Cox) test. Dil., dilution; Nabs, neutralizing Abs; Sp., specific.

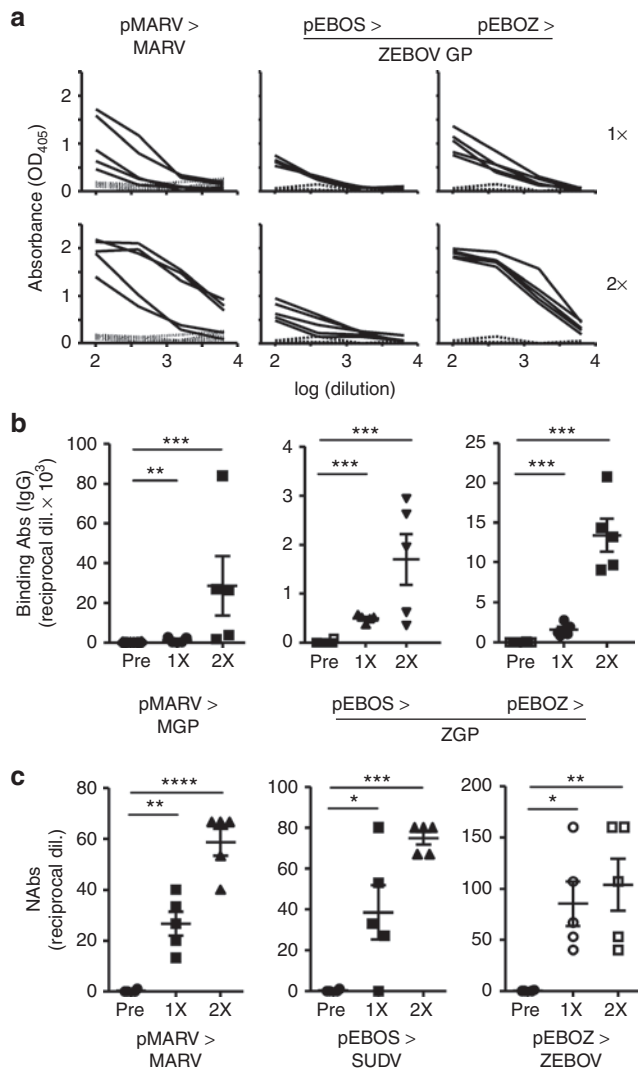


**Figure 3** Induction of neutralizing Abs. B cell responses were assessed in mice ( $n = 5/\text{group}$ ) 20 days following each of two vaccinations, spaced 3 weeks between injections with  $40 \mu\text{g}$  of E-DNA vaccination. Serum GP-specific IgG responses from vaccinated (solid lines) mice or pre-bleed (dotted lines) mice were (a) measured by ELISA and (b) summarized. All responses from pEBOS- and pEBOZ-immunized animals were measured against sucrose-purified ZGP, as SGP was not available for this study. IgG responses from pMARV-immunized mice were measured against MARV-Ozolin GP or with negative control sucrose-purified Nipah G protein. (c) Neutralization activity of serum samples was measured against ZEBOV-EGFP, SUDV-Boniface, and MARV-Angola in a BSL-4 facility and NAb titers are shown. NAbs against SUDV-Boniface were assayed based on cytopathic effect (CPE) on CV-1 cells and those against MARV-Angola were assayed using an immunofluorescent assay. (b,c) Averages are shown and error bars represent SEM. Group analyses were completed by matched, two-tailed, unpaired  $t$ -test. Experiments were repeated at least two times with similar results and  $*P < 0.1$ ;  $**P < 0.01$ ;  $***P < 0.001$ . Dil., dilution; GP, glycoprotein; Nabs, neutralizing Abs.

and then boosted with the same vaccines 1 month later. Animals were challenged 28 days following the second immunization with 1,000 LD<sub>50</sub> of a guinea pig-adapted MARV-Angola (gpMARV) ( $n = 9$ ) or ZEBOV (gpZEBOV) ( $n = 15$ ) in a BSL-4 facility, and then observed and weighed daily (Figure 2). Vaccinated animals were completely protected, whereas control-vaccinated animals

succumbed to gpMARV by 10 days after challenge ( $n = 3$ ;  $P = 0.0052$ ) or to gpZEBOV by day 7 after challenge ( $n = 6$ ;  $P = 0.0008$ ) (Figure 2a,e). In addition, vaccinated animals were protected from weight loss (Figure 2b,f;  $P < 0.0001$ ). It is likely that vaccine-induced Abs may have contributed to protection, because GP-specific Abs in pooled serum exhibited a significant increase in binding (Figure 2c,g) and neutralization (Figure 2d,h) titers.

### Plasmid vaccines were highly immunogenic

To better characterize immune correlates as driven by the protective E-DNA vaccine, we next used the mouse model which has been widely used as a screening and “proof-of-concept” tool for filoviral vaccine development (Supplementary Note S4),<sup>4</sup> and in which extensive immunodetection reagents are available. First, B-cell responses were assessed in H-2<sup>d</sup> mice ( $n = 5/\text{group}$ ) 20 days following each of two vaccinations, 3 weeks between injections with  $40 \mu\text{g}$  of respective monovalent E-DNA vaccine (Figure 3). Although little GP-specific IgG was observed in pre-bleed control samples, a significant increase was detected in all animals following vaccination (Figure 3a,b). As purified SUDV GP (SGP) was not available, purified ZGP was used as a surrogate. IgG in SUDV-vaccinated mice bound ZGP, demonstrating the ability for vaccine-induced Ab generation as well as its capability for cross-species recognition. In addition, seroconversion occurred in 100% of vaccinated animals after only one immunization, after which responses were significantly increased by homologous boost; average reciprocal endpoint dilution titres were boosted 22.1-fold in pMARV-immunized mice, and 3.4- and 8.6-fold in pEBOS- and pEBOZ-vaccinated animals, respectively. Samples were next assayed for neutralization of ZEBOV, SUDV-Boniface, and MARV-Angola in a BSL-4 facility (Figure 3c), and significant increases in NAb titres were detected following vaccination in all animals.

Mice from two different genetic backgrounds (H-2<sup>d</sup> and H-2<sup>b</sup>;  $n = 5/\text{group}$ ) were immunized with  $40 \mu\text{g}$  of respective E-DNA, homologous boosted after 2 weeks, and then T-cell analysis was performed 8 days later (Figure 4). We developed a novel modified ELISPOT assay to assess the comprehensive vaccine-induced T-cell response, in which splenocytes were stimulated using individual peptides as opposed to matrix pools (Figure 4a).<sup>21</sup> E-DNA vaccination induced robust IFN $\gamma$ <sup>+</sup> responses that recognized a diversity of T-cell epitopes (Table 1). All positive epitope-comprising peptides were subsequently gated (Supplementary Figure S1), confirmed, and further characterized by FACS (data not shown). This modified ELISPOT approach proved extremely sensitive, because background responses from control wells were low ( $7.2 \pm 0.2$  IFN $\gamma$ -producing SFC/10<sup>6</sup> splenocytes in H-2<sup>b</sup> and  $9.2 \pm 0.5$  in H-2<sup>d</sup> mice). Results showed that vaccination with pMARV induced 9 measurable epitopes in H-2<sup>b</sup> mice and 11 in H-2<sup>d</sup>, pEBOS induced 9 and 8, and pEBOZ generated 10 and 12, in these respective strains (Figure 4a). Although five of nine (55.6%) of the epitopes from pMARV-immunized H-2<sup>b</sup> mice were CD8<sup>+</sup>, they accounted for about 57.3% of the total MGP-specific IFN $\gamma$ <sup>+</sup> response as measured by both ELISPOT and FACS confirmation and phenotypic analysis (data not shown). Similarly, only 33% and 38% of confirmed epitopes were CD8-restricted in pEBOS-immunized H-2<sup>b</sup> and H-2<sup>d</sup> mice, respectively. However,

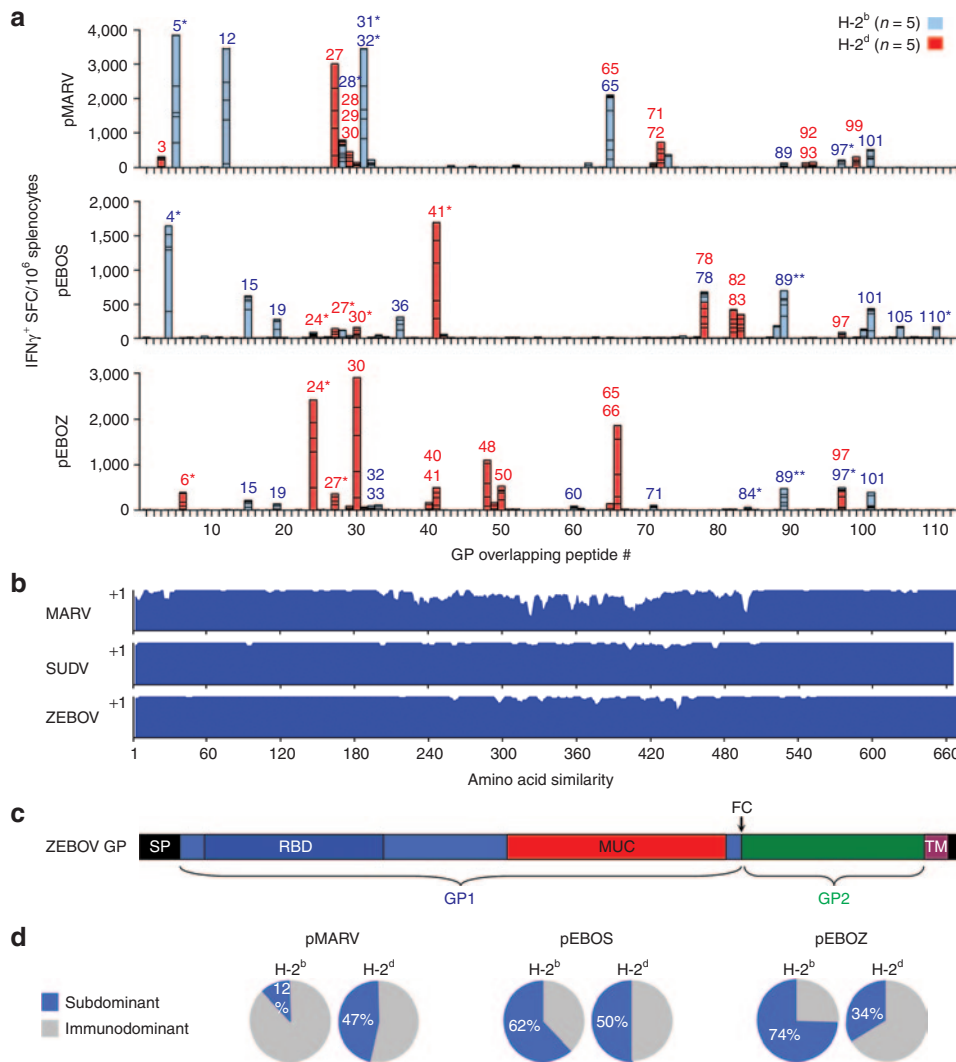


**Figure 4 Vaccination generated broad T cells. (a)** H-2<sup>b</sup> (blue bars) and H-2<sup>d</sup> (red bars) mice ( $n = 5$ /group) were immunized twice with either pMARV, pEBOS or pEBOZ E-DNA, and IFN $\gamma$  responses were measured by modified IFN $\gamma$  ELISPOT assay developed herein. Splenocytes harvested 8 days after the second immunization were incubated in the presence of individual GP peptides (15-mers overlapping by 9 amino acids) and results are shown in stacked bar graphs. Epitope-containing peptides were identified ( $\geq 10$  average spots and  $\geq 80\%$  response rate), confirmed by flow cytometry and characterized in the population of total activated IFN $\gamma$ <sup>+</sup> and CD44<sup>+</sup> CD4<sup>+</sup> and/or CD8<sup>+</sup> T cells (Table 1), and peptide numbers of positive inducers are indicated above the bars. Peptides containing CD4<sup>+</sup> epitopes alone, \*CD8<sup>+</sup> epitopes alone, and dual CD4<sup>+</sup> and \*\*CD8<sup>+</sup> epitopes are indicated. Putative shared and/or partial epitopes were explored for contiguous positive peptide responses (Table 1). **(b)** Amino acid similarity plots comparing GP sequences from MARV, SUDV, and ZEBOV viruses displayed in Figure 1a. **(c)** Cartoon displaying putative domains within the ZEBOV GP (GenBank #VGP\_EBOZM). **(d)** Total subdominant (blue) and immunodominant (gray) T-cell epitopic responses are displayed as a percentage of the total IFN $\gamma$  response generated by each vaccine. Experiments were repeated at least two times with similar results. FC, furin cleavage site; GP, glycoprotein; MUC, mucin-like region; RB, receptor binding; SP, signal peptide; TM, transmembrane region.

these epitopes comprised roughly 50–90% of the total response; CD8<sup>+</sup> T-cell responses were estimated to be ~56% in both mouse strains, whereas FACS estimates were 51% and 90% in H-2<sup>b</sup> and H-2<sup>d</sup> mice, respectively. Total CD8<sup>+</sup> responses were lower in pEBOZ-vaccinated animals and measured between 33% and 57% (33% for both strains by ELISPOT and 6% and 57% for H-2<sup>b</sup> and H-2<sup>d</sup> mice, respectively, by FACS).

A single immunodominant epitope was detected in both mouse strains receiving pEBOS where an immunodominant epitope was loosely defined as generating an IFN $\gamma$  response at least twofold over the highest subdominant epitope; pMARV induced four H-2<sup>b</sup>-restricted immunodominant CD8<sup>+</sup> epitopes within

peptides MGP<sub>25–39</sub> (#5), MGP<sub>67–81</sub> (#12), MGP<sub>181–195</sub> (#31), and MGP<sub>385–399</sub> (#65), and an H-2<sup>d</sup>-restricted CD4<sup>+</sup> epitope in MGP<sub>151–171</sub> (#27). Four of these epitopes occurred within highly conserved regions of MARV GP1, including three of which were located within the putative receptor binding domain, whereas only one occurred within the variable mucin-like region (MGP<sub>385–399</sub> (#65)) (Figure 4b,c). pEBOS-stimulated CD8<sup>+</sup> epitopes occurring in SGP<sub>19–33</sub> (#4) and SGP<sub>241–255</sub> (#41) in H-2<sup>b</sup> and H-2<sup>d</sup> mice, respectively, both in highly conserved regions of GP1. However, pEBOZ immunization revealed three immunodominant epitopes in H-2<sup>d</sup> mice (a CD8-restricted epitope located in the ZEBOV GP receptor binding domain (GP)<sub>139–153</sub> (#24), and two CD4-restricted

Table 1 Identification and characterization of vaccine-induced T-cell epitopes<sup>a</sup>

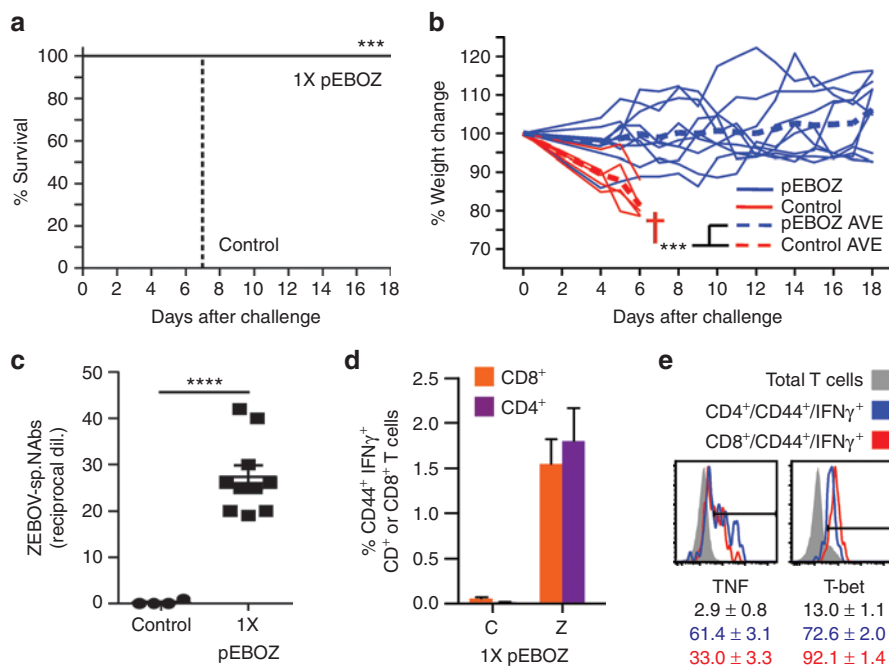
Enhanced plasmid vaccine	GP sequence	Pep #	Position	Sequence	H-2	ELISPOT		FACS T-cell restriction	Best con. % rank (IEDB)					Previously defined (80% Blast; Allele)	
						AVE	±SEM		CD8 <sup>+</sup> (≤0.5)	I-A <sup>b</sup>	I-A <sup>d</sup>	I-E <sup>d</sup>	CD4 <sup>+</sup> (<25)		
pMARV	MARV <sub>ANG</sub>	3	13-27	IQGVKTLPILEIASN	d	62	34	4+					12.1		
		5	25-39	ASNIQPNVDVSCSG	b	743	186	8+	0.4						
		12	67-81	SKRWAFRAGVPPKNV	b	694	204	4+		0.8					
		27	157-171	GKVFTEGNIAAMIVN	d	602	75	4+		12.9					
		28	163-177	GNIAAMIVNKTIVHKM	b/d	126	28	8+	0.2				3.9		
				GNIAAMIVNKTIVHKM	d	30	10	4+	0.2				3.9		
		29	169-183	IVNKTIVHKMIFSRQG	d	92	17	4+					17.2		
		30	175-189	HKMIFSRQGGYRHM	d	31	10	4+					23.9		
		31	181-195	RQGGYRHMNI <del>LT</del> STN	b	674	112	8+	0.1						
		32	187-201	RHMNI <del>LT</del> SNKYWTSS	b	44	16	8+							
		65	385-399	LPTE <del>NP</del> TTAKSTNST	b/d	398/16	107/2	4+					24.0		
71	421-435	PNSTAQHLVYFRKR	d	29	6	4+						7.5	H-2 <sup>d</sup> class I <sup>p</sup>		
72	427-441	HLVYFRKRNI <del>LW</del> RE	d	145	18	4+						8.3			
89	529-543	GLSWIPFFGPGIEGL	b	26	8	4+			0.3		7.0				
92	547-561	GLIKNQNNLVCLRR	d	29	10	4+						13.3			
93	553-567	NNLVCLRRLANQTA	d	34	13	4+									
97	577-591	TTEERTFSLNRRHAI	b	46	18	8+	0.1								
99	589-603	HAIDFLARWGGTCK	d	63	12	4+							21.8		
101	601-615	TKVLGPPCCIGIED	b	97	37	4+			0.4						
pEBOS	SUDV <sub>CON</sub>	4	19-33	FFVWVHILFQKAFSM	b	310	139	8+	0.4						
		15	85-99	RWGRSGVPPKVVSY	b	108	59	4+				1.2			
		19	109-123	YNLEIKKPDGSECLP	b	55	25	4+							
		24	139-153	HKAQGTGPCPGDYAF	d	13	3	8+			0.3				
		27	157-171	GAFLYDRLASTVIY	d	29	9	8+				21.1		23.4	
		30	175-189	NFAEGVIAFLILAKP	d	31	6	4+							
		36	211-225	SYA <del>T</del> SYLEYEIE <del>N</del> F	b	60	16	4+	0.4		0.1				
		41	241-255	FVLLDRPHTPQELFQ	d	338	55	8+			0.3	0.1			
		78	463-477	NITTA <del>V</del> KTVLPQEST	b/d	28/105	12/18	4+					7.2		
		82	487-501	TGILGSLGLRKR <del>RR</del>	d	82	14	4+							17.2
		83	493-507	LGLRKR <del>RR</del> QVNTRA	d	69	12	4+							
89	529-543	IAWIPYFGPGAEGYI	b	123	40	8+/4+			0.1		3.0		H-2 <sup>b</sup> class I <sup>10</sup>		
97	577-591	TELRTY <del>T</del> ILNRKAID	d	12	5	4+	0.1								
101	601-615	CRILGPDCCIEPHDW	b	80	41	4+									
105	625-639	QIHDFIDNPLPNQD	b	28	23	4+							0.3		
110	655-669	GIGTGHIAI <del>IA</del> LL	b	27	19	8+									

Table 1 Continued on next page

Table 1 Continued

Enhanced plasmid vaccine	GP sequence	Pep #	Position	Sequence	H-2	ELISPOT		FACS T-cell restriction	Best con. % rank (IEDB)							Previously defined (80% Blast; Allele)	
						AVE	±SEM		CD8 <sup>+</sup> (≤0.5)			CD4 <sup>+</sup> (<25)					
									D <sup>b</sup>	K <sup>b</sup>	D <sup>d</sup>	K <sup>d</sup>	L <sup>d</sup>	I-A <sup>d</sup>	I-E <sup>d</sup>		
pEBOZ	ZEBOV <sub>CON</sub>	6	31-45	FSIPLGVIHNSLQV	d	78	31	8+					0.2				
		15	85-99	RWGRSGVPPKVVNY	b	44	12	4+		1.2							
		19	109-123	YNLEIKKPDGSECLP	b	29	12	4+									
		24	139-153	HKVSGTGPCAGDEAF	d	484	85	8+					0.1	14.9			H-2 <sup>d</sup> class I <sup>10,48</sup>
		27	157-171	GAFFLYDRLASTVIY	d	72	18	8+						21.1		23.4	H-2 <sup>d</sup> class I <sup>7,49</sup>
		30	175-189	TEAEGVVAFLLPQA	d	581	85	4+			0.2				21.6		
		32	187-201	PQAKKDFSSHPLRE	b	18	6	4+	0.1	0.4				16.4			
		33	193-207	FFSSHPLREPVNATE	b	21	8	4+						14.7			
		40	235-249	EVDNLTYYVQLESRFT	d	32	17	4+			0.4				19.6		
		41	241-255	YVQLESRFTPQFLIQ	d	97	23	4+									
		48	283-297	TTIGEWAFWETKKNL	d	219	70	4+								12.9	
		49	289-303	AFWETKKNLTKIRS	d	32	15	4+								22.9	
		50	295-309	KNLTRKIRSEELSFT	d	105	37	4+							22.7		
		60	355-369	SQGREAAVSHLTLA	b	16	7	4+	0.3					23.1	3.9		
		65	385-399	DNSTHNTPVYKLDIS	d	29	18	4+									
		66	391-405	TPVYKLDISEATQVE	d	371	118	4+									
		71	421-435	PPATTAAGPPKAENT	b	21	8	4+						22.6	5.5		
		84	499-513	TRREAVNAQPKCNP	b	12	5	8+	0.3					14.6	7.9		
		89	529-543	LAWIPYFGPAAEGYI	b	93	8	8+/4+			0.1			0.8			H-2 <sup>b</sup> class I <sup>7,10</sup>
		97	577-591	TELRTEFSLNRKKAID	b/d	14/82	4/42	8+	0.1							22.2	H-2 <sup>b</sup> class I <sup>30</sup>
		101	601-615	CHILGPDCCIEPHDW	b	96	62	4+									

\*Epitope-containing peptides were identified by IFN $\gamma$  ELISPOT ( $\geq 10$  SFC/10<sup>6</sup> splenocytes and  $\geq 80\%$  response rate) and then confirmed by FACS ( $\geq 3-5 \times 10^4$  CD3<sup>+</sup> cells were acquired). Responses for each were further characterized by FACS (expression of CD4 and/or CD8 by CD3<sup>+</sup>/CD44<sup>+</sup>/IFN $\gamma$ <sup>+</sup> cells). Predicted CD8<sup>+</sup> epitopes are underlined (best consensus % rank by IEDB) and previously described epitopes are referenced. Immunodominant epitopes are displayed (\*).



**Figure 5** Protective “single-dose” vaccination induced neutralizing Abs and CTL. H-2<sup>k</sup> mice ( $n = 10/\text{group}$ ) were vaccinated once i.m. with pEBOZ E-DNA and then challenged 28 days later with 1,000 LD<sub>50</sub> of mZEBOV in a BSL-4 facility. Mice were weighed daily and monitored for disease progression. **(a)** Animal survival data and **(b)** % change in body weight are displayed for immunized (solid black or blue lines, respectively) and control animals (dashed or solid red lines, respectively). Average body weight is also displayed as dashed lines in **b**. **(c)** NAbs measured before challenge. **(d)** T-cell responses after a single pEBOZ immunization as measured by FACS are summarized as average % of total CD44<sup>+</sup>/IFN $\gamma$ <sup>+</sup> CD4<sup>+</sup> (purple) or CD8<sup>+</sup> (orange) cells. **(e)** T<sub>H</sub>1-type effector markers were assessed (TNF and T-bet) and data for CD44<sup>+</sup>/IFN $\gamma$ <sup>+</sup> CD4<sup>+</sup> (blue) and CD8<sup>+</sup> (red) T cells are overlaid on total T-cell data (dashed). \*\*\* $P < 0.001$ ; \*\*\*\* $P < 0.0001$ . Group analyses were completed by matched, two-tailed, unpaired  $t$ -test and survival curves were analyzed by log-rank (Mantel–Cox) test and daggers (†) denote animals that succumbed to disease. Experiments were performed twice with similar results and error bars represent SEM. Dil., dilution; Nabs, neutralizing Abs; Sp., specific.

epitopes ZGP<sub>175–189</sub> (#30) and ZGP<sub>391–405</sub> (#66), occurring within the receptor binding domain and the mucin-like region, respectively. Only one immunodominant epitope was defined in H-2<sup>b</sup> mice which contained both a CD4<sup>+</sup> and a CD8<sup>+</sup> epitope (#89) and occurred in a highly conserved region of GP2. Overall, diverse epitope hierarchies were consistent and reproducible in each vaccine group. Furthermore, the subdominant response comprised a significant proportion of the total response (**Figure 4d**); the total average subdominant response as measured by the modified ELISPOT assay was ~12, 62, and 74% in pMARV-, pEBOS- and pEBOZ-immunized H-2<sup>b</sup> mice, respectively, whereas responses in H-2<sup>d</sup> mice were 47, 50, and 34%, respectively.

Lastly, total GP-specific T-cell responses were measured by FACS using stimulation with minimal peptide pools containing only confirmed epitope-comprising peptides identified above (**Supplementary Figure S2**). Robust responses were detected in each of the vaccinated animals and were, in a majority of cases, comprised by both activated CD4<sup>+</sup> and CD8<sup>+</sup> T cells. Responses were GP-specific, because little IFN $\gamma$  production was observed with a control peptide (h-Clip), and correlated well with ELISPOT data. The only instance where immunization did not induce remarkable CTL as measured by FACS was in H-2<sup>d</sup> mice vaccinated with pMARV in which no epitope identified by ELISPOT was confirmed to be CD8-restricted. Altogether, these data show that each of the vaccine plasmids was highly immunogenic in mice and yielded robust GP-specific T-cell responses recognizing a diverse array of T-cell epitopes including immunodominant

epitopes within highly conserved regions of the GP. Furthermore, the highly diverse subdominant T-cell response characterized herein might have otherwise been overlooked using traditional matrix array peptide pools for epitope identification.

### “Single-dose” protection in mice

Vaccine efficacy against ZEBOV challenge was next assessed in the preclinical murine model (**Supplementary Note S4**);<sup>4</sup> however, mice were vaccinated only once due to strong NAb induction and protection data above. Mice (H-2<sup>k</sup>;  $n = 10/\text{group}$ ) were immunized with 40  $\mu\text{g}$  of the pEBOZ E-DNA and protection was evaluated 28 days later by challenge with 1,000 LD<sub>50</sub> of mouse-adapted ZEBOV (mZEBOV) in a BSL-4 facility. Although all control animals succumbed to infection by day 7 after challenge, E-DNA-vaccinated mice were completely protected (**Figure 5a**;  $P = 0.0002$ ). In addition, control mice exhibited progressive loss of body weight until death (**Figure 5b**;  $P < 0.0001$ ).

To better understand the mechanisms of E-DNA-induced protection in a “single-dose” model, we next assessed NAb and T-cell generation. NAbs were assessed 25 days after vaccination, 3 days before challenge, and a significant ( $P < 0.0001$ ) increase was detected in all vaccinated animals ( $n = 10/\text{group}$ ); reciprocal endpoint dilution titers ranged from 19 to 42,  $27.3 \pm 2.5$  (**Figure 5c**). We next evaluated the generation of ZGP-specific T cells and increased the scope of our analysis to compare responses in mice immunized with either the pEBOZ alone, or in a trivalent formulation (**Supplementary Figure S3**). IFN $\gamma$  production ( $n = 5$ ) was assessed

11 days later by FACS using whole ZGP peptide pools (Figure 5d). IFN $\gamma$ -producing T cells were detected in all animals and were specific for ZGP peptides, because stimulation with a control peptide did not induce cytokine production. Immunization with either the monovalent or trivalent formulation induced robust IFN $\gamma$  T-cell responses that, when compared, were not significantly different (Supplementary Figure S3;  $P = 0.0920$ ).

As CTL may be important in eliminating virus-infected cells,<sup>7,9-12</sup> production of an additional effector cytokine, TNF, as well as a developmental restriction factor, T-box transcription factor TBX21 (T-bet), known to correlate with T<sub>h</sub>1-type CTL immunity and cytotoxicity<sup>24</sup> were measured (Figure 5e). We found that ~61% and ~33% of activated CD4<sup>+</sup> and CD8<sup>+</sup> T cells, respectively, also produced TNF in addition to IFN $\gamma$ . Furthermore, a majority of IFN $\gamma$ -producing T cells expressed high levels of T-bet; about 73% and 92% of CD8<sup>+</sup> and CD4<sup>+</sup> T cells, respectively, were T-bet<sup>+</sup>, CD44<sup>+</sup>, and produced IFN $\gamma$  following ZGP peptide stimulation.

## DISCUSSION

We report development and evaluation of a polyvalent-filoviral vaccine in preclinical rodent immunogenicity and efficacy studies. Complete protection against challenge with gpMARV and gpZEBOV was observed following two E-DNA vaccine doses in guinea pigs, as well as with a “single-dose” E-DNA vaccine in mice against mZEBOV (Figures 2 and 5). To date, genetic vaccination of guinea pigs has included either injection of naked DNA<sup>25</sup> or DNA delivered by gene gun;<sup>26-28</sup> however, either method required at least three vaccinations to achieve complete protection. Improved protection herein may be due to the induction of robust Abs, because a single E-DNA vaccination generated GP-specific IgG binding titers that were comparable in magnitude with titers in protected animals following gene gun administration;<sup>28</sup> E-DNA vaccination induced 3.85 and 2.18 log<sub>10</sub> ZGP and MGP-specific Ab titers, respectively, after a single administration versus 2.7 and 3.0 after three gene gun vaccinations. For comparison with an alternative “single-dose” protective strategy in guinea pigs, a Ag-coupled virus-like particle platform generated Ab titers that were only slightly higher than observed following E-DNA vaccination.<sup>29</sup> Furthermore, a recombinant adenovirus approach induced ZGP-specific NAb titers that were lower than those from a single E-DNA vaccination (53 reciprocal endpoint dilution titer versus 88 herein).<sup>30</sup> Vaccination with recombinant vesicular stomatitis viruses<sup>31</sup> generated ZGP-specific Ab titers that were similar to the current platform. Altogether, these data demonstrate that E-DNA vaccination was capable of inducing binding and neutralizing Abs that were comparable with non-replicating viral platforms and that these data may help, in part, to explain strong guinea pig survival data herein.

The generation of NAbs by protective E-DNA vaccination may have benefitted by transgene-expressed mature GP structures. *In vitro* transfection studies confirmed that the vaccine-encoded GP were highly expressed, post-translationally cleaved (Figure 1b), transported to the cell surface, and sterically occluded the immunodetection of cell surface molecules (Figure 1c).<sup>23</sup> Therefore, it was highly likely that the vaccine immunogens formed herein matured into hetero-trimeric spikes that would otherwise be functional upon virion assembly during infection. This may be important for the generation and display of virologically relevant neutralizing

determinants which would be subsequently critical for the induction of conformation-dependent NAbs.<sup>32,33</sup> Thus, in this regard, the expression of native anchored structures may be superior to soluble derivatives in the capacity for generating NAbs.<sup>34,35</sup>

To better characterize T-cell responses as driven by a protective vaccine, we performed immunogenicity and efficacy studies in mice and determined “single-dose” complete protection against mZEBOV with E-DNA vaccination (Figure 5). To date, the most effective platforms conferring complete protection in this model are virus-like particle, either with<sup>7,36</sup> or without<sup>37</sup> adjuvant, recombinant adenovirus vaccination,<sup>30,38,39</sup> or rRABV vaccination.<sup>40</sup> However, characterization of T-cell responses were severely limited in these studies and were restricted to splenocyte stimulation with either two<sup>36</sup> or one<sup>7</sup> peptides previously described to contain ZGP T-cell epitopes.<sup>7,10,30,38,39</sup> Herein, we report induction of robust and broad CTL by protective vaccination as extensively analyzed by a novel modified T-cell assay (Figure 4a and Table 1).<sup>21</sup> In total, 52 novel T-cell epitopes were identified including numerous immunodominant epitopes occurring primarily in highly conserved regions of GP. Of the 22 total ZGP epitopes identified, only 4 have been previously reported.<sup>7,10</sup> Moreover, only 1 of the 20 MGP<sup>9</sup> and 1 of 16 SGP epitopes were previously described. As such, this the most comprehensive report of preclinical GP epitopes to date, describing GP epitopes from multiple filoviruses in two different mouse genetic backgrounds.<sup>4,9,10</sup>

Another novel finding resulting from these analyses was the assessment of the vaccine-induced subdominant T-cell responses, which we show comprised a significant percentage of the total T-cell response, widely ranging between 12 and 74% (Figure 4d). This may be particularly important because the subdominant responses can significantly contribute to protection.<sup>41,42</sup> Thus, it may prove informative in the future to determine the specific contributions of the subdominant and immunodominant epitopic T-cell responses to protection.<sup>32</sup> Notably, these responses may have otherwise been overlooked using traditional matrix array peptide pools for epitope identification.<sup>32</sup> As such, limited epitope detection in previous studies may have been directly related to lower levels of vaccine-induced immunity, the use of less sensitive standard assays, and/or the use of peptide arrangements and/or algorithms favoring detection of immunodominant CD8<sup>+</sup> epitopes.

Although immune correlates of protection against the filoviruses remain controversial, data generated by this highly immunogenic approach provide a unique opportunity with which to study T-cell immunity as driven by a protective vaccine. E-DNA vaccination herein induced strong ZGP-specific T cells, a large part of which were characterized by T<sub>h</sub>1-type multifunctional CTL expressing high levels of T-bet (Figure 5f), also shown to correlate with T-cell cytotoxicity in humans.<sup>24</sup> It is clear that previous stand-alone DNA vaccine platforms capable of generating mainly humoral immune responses and cellular immunity skewed towards CD4<sup>+</sup> T cells may likely benefit from *in vivo* electroporation delivery which has been recently demonstrated to induce potent CD8<sup>+</sup> T cells in nonhuman primates and the clinic.<sup>12,18-20</sup> Thus, data herein strongly support further evaluation of this approach as a stand-alone or prime-boost modality in non-human primate immunogenicity and efficacy studies. Specifically, the induction and composition of the CD4<sup>+</sup> and CD8<sup>+</sup> effector

T-cell response, capacity for T-cell cross-reactivity among divergent GP, and expression of cytolytic function<sup>4</sup> should be explored. This approach offers an attractive vaccination strategy that can be quickly and inexpensively modified and/or produced for rapid response during *Filoviridae* bio-threat situations and outbreaks. In addition, this model approach provides an important tool for studying protective immune correlates against filoviral disease and could be applied to existing platforms to guide future strategies.

## MATERIALS AND METHODS

**Plasmid vaccine construction.** The pMARV, pEBOS, and pEBOZ plasmid DNA constructs encode full-length GP proteins. An amino acid consensus strategy was used for the pEBOS and pEBOZ, whereas a type-matched sequence from the 2005 Angola outbreak strain was used (GenBank #VGP\_MABVR) for pMARV.<sup>22</sup> Consensus sequences were determined by alignment of the prevailing ZEBOV and SUDV GP amino acid sequences and generating a consensus for each. Each vaccine GP gene was genetically optimized for expression in humans (including codon- and RNA-optimization, among other proprietary modifications for enhancing protein expression (GenScript, Piscataway, NJ)), synthesized commercially, and then subcloned (GenScript) into modified pVAX1 mammalian expression vectors (Invitrogen, Carlsbad, CA) under the control of the cytomegalovirus immediate-early promoter; modifications include 2A>C, 3C>T, 4T>G, 241C>G, 1,942C>T, 2,876A>-, 3,277C>T, and 3,753G>C. Phylogenetic analysis was performed by multiple-alignment with ClustalW using MEGA version 5 software (<http://www.megasoftware.net>).

In developing a strategy to provide protection against multiple species responsible for the highest human case-fatality rates, we focused on MARV, SUDV, and ZEBOV. Due to their relative divergence, we hypothesized that development of a polyvalent-filovirus vaccine would require a cocktail of components that can be quickly and easily adapted in response to future outbreak strains and/or species. Although overall diversity among the EBOV is about 33%, amino acid identity increases substantially when SUDV and ZEBOV are analyzed separately (~94% identity within each species). Therefore, we chose a two component strategy for coverage of the most lethal EBOV, one plasmid GP vaccine for SUDV and another for ZEBOV (Figure 1a). As GP diversity among each species was relatively low (5.6% for SUDV and 7.1% for ZEBOV), consensus immunogens were developed to increase interspecies coverage, a strategy shown previously to enhance protection among divergent strains of influenza and HIV.<sup>43,44</sup> These GP sequences were consensus for all reported outbreak sequences (GenBank) as determined by alignment using Vector NTI software (Invitrogen; Figure 1a). Non-consensus residues, four amino acids each in SUDV (95, 203, 261, and 472) and ZEBOV (314, 377, 430, and 440), were weighted towards Gulu and Mbomo/Mbanza, respectively. Gulu was chosen as it was responsible for the highest human case-fatality rate of any *Filoviridae* outbreak ( $n = 425$ ), whereas Mbomo/Mbanza was chosen as they were the most recent and lethal outbreaks with published sequence data. The consensus GP for SUDV (SUDV CON VACCINE) and ZEBOV (ZEBOV CON VACCINE) were phylogenetically intermediary their parentally aligned strains (Figure 1a). Alternatively, GP diversity among the MARV was much higher (~70% identity) in comparison, so a consensus strategy was not adopted. For coverage of MARV, we chose to use the MGP sequence from the 2005 outbreak in Angola (GenBank #VGP\_MABVR), because it was solely responsible for the largest and deadliest MARV outbreak to date ([http://www.cdc.gov/ncidod/dvrd/spb/mnpages/dispages/fact\\_sheets/fact\\_sheet\\_marburg\\_hemorrhagic\\_fever.pdf](http://www.cdc.gov/ncidod/dvrd/spb/mnpages/dispages/fact_sheets/fact_sheet_marburg_hemorrhagic_fever.pdf)).<sup>22</sup> This sequence was >10% divergent from either of its closest cluster of relative strains including Musoke, Popp, and Leiden (10.6% divergence), or Uganda (01Uga07), Durba (05DRC99 and 07DRC99), and Ozolin (10.3% divergence). Altogether, a three-plasmid strategy formed the foundation for our novel trivalent polyvalent-filovirus vaccine strategy.

**GenBank protein IDs.** Identification of proteins in Figure 1a are as follows: MARV Durba (05DRC99) '99: ABE27085; Uganda (01Uga07) '07: ACT79229; Durba (07DRC99) '99: ABE27078; Ozolin '75: VGP\_MABVO; Musoke '80: VGP\_MABVM; Popp '67: VGP\_MABVP; Leiden '08: AEW11937; Angola '05: VGP\_MABVA; Ravn '87: VGP\_MABVR; Durba (09DRC99) '99: ABE27092; Uganda (02Uga07) '07: ACT79201. SUDV: Boniface '76: VGP\_EBOSB; Maleo '79: VGP\_EBOSM; Yambio '04: ABY75325; Gulu '00: VGP\_EBOSU. ZEBOV: Booue '96: AAL25818; Mayibout '96: AEK25495; Mekouka '94: AAC57989, VGP\_EBOG4; Kikwit '95: VGP\_EBOZ5; Yambuku (Ekron) '76: VGP\_EBOEC; Yambuku (Mayinga) '76: VGP\_EBOZM; Kasai '08: AER59712; Kasai '07: AER59718; Etoumbi '05: ABW34742; Mbomo/Mbandza '03: ABW34743.

### Filoviral vaccine GP immunogen sequences

*Zaire ebolavirus* consensus (ZEBOV CON VACCINE; pEBOZ): MGVTGILQ LPRDRFKRTSFFLWVILFQRTFSIPLGVIHNSLTQVSDVDKLVCRD KLSSTNQLRSVGLNLEGNVATDVPASPATKRWGFRSGVPPKVVN YEAGWAENCYNLEIKKPDGSECLPAAPDGIRGFPCRYVHKVSGT GPCAGDFAFHKEGAFFLYDRLASTVIYRGTTFAEGVVAFLILPQAK KDFFSSHPLREPVNATEDPSSGYSTTIRYQATGFGTNETEYLFVVDNL TYVQLESRFTQPFLQLNETIYTSKGKRSNTTGKLIWKVNPEIDTTIGE WAFWETKKNLTKRIRSEELSFTAVSNRAKNISGQSPARTSSDPGTNTT TEDHKIMASENSSAMVQVHSQGREAAVSHLTLTATISTSPQSPPTTKP GPDNSTHNTPVYKLDISEATQVEQHRRRTDNDSTASDTPPATTAAGP PKAENTNTSKSTDLLDPATTTSPQNHSETAGNNNTHHQTGEESSASS GKLGLTNTIAGVAGLITGRRRTREAIVNAQPKCNPNLHYWTTQDE GAAIGLAWIPYFGPAEAGIYTEGLMHNQDGLICGLRQLANETTQALQL FLRATTELRTFSILNRKAIIDFLLRQWGGTCHILGPDCCIEPHDWTKNIT DKIDQIHDHFVDKTLDPDQGDNDNWWTGWRQWIPAGIGVTGVIIAVI ALFCICKFVF

*Sudan ebolavirus* consensus (SUDV CON VACCINE; pEBOS): MEGLSLLQLPRDKFRKSSFFVWVILFQKAFSMLPGVVTNSTLEV TEIDQLVCKDHLASTDQLKSVGLNLEGGVSTDIPSATKRWGFRS GVPKVVSYEAGWAENCYNLEIKKPDGSECLPPPPDGVRGF PRCRYVHKAQGTGCPGDYAFHKDGAFFLYDRLASTVIYRVN FAEGVIAFLILAKPKETFLQSPPIREAVNTSSYATSYLGEYI ENFGAQHSTTLFKINNNTFVLLDRPHTPQLFLQNDTIHLHQQL SNTTGKLIWTL DANINADIGEWAFWENKKNLSEQLRGEELS FETLSLNETEDDDATSSRTTKGRISDRATRKYSDLVPKDSGPMVSL HVPEGETTLPQNSTEGRRVDVNTQETITETTATIHTNGNMQ ISTIGTGLSSQILSSSPTMAPSPETQTSTTYTKPLPVMTEEPTTP PRNSPGSTTEAPTLTTPENITTAVKTVLPQUESTSNGLITSTVTGILG SLGLRKRSRVNRATGKCNPNLHYWTAQEQHNAAGIAWIPYF GPAGEIYTEGLMHNQALVCLRQLANETTQALQLFLRATTEL RYTIILNRKAIIDFLLRWGGTCRILGPDCCIEPHDWTKNITDKIN QIHDHFIDNPLPNQDNDNWWTGWRQWIPAGIGITGIIIALL CVCKLLC

*Marburg marburgvirus* Angola (MARV VACCINE; pMARV): MKTTCLLISLILIQGVKTLPILEIASNIQPQNVDSVCSGTLQKT EDVHLMGFTLSGQKVADSPLEASKRWAFRAGVPPKNVEYTE GEEAKTCYINISVTDPSGKSLLDPTNIRDYPKCKTIHHIQGN PHAQGIALHLWGAFFLYDRIASTMYRGKVFTEGNIAAMI VNKTVHKMIFSRQGGYRHMNLTSTNKYVWSSNGTQNTNDT GCFGLTQEYNSTKNQTCAPSKKPLPLPTAHPEVKLTSTSDAT KLNTTDPNSDDEDLTTSGSGSGEQEPYTTSDAATKQGLSSTMPPTP SPQPSTPQQGNNNTNHSQGVVTEPGKNTTAQPSMPPHNTT TISTNNTSKHNLSTPSVPIQATNNTYNTQSTAPENEQTSAPSKTTLT TENPTTAKSTNSTKSPTTTPVNTTNKYSTSPSTPNSTAQHLVY FRRKRNLWREGDMFPFLDGLINAPIDFDPVNTKTIFDESSS GASAEEDQHASPNSILTSYFPKVNENTAHSGENENDCDAELRIW SVQEDDLAAGLSWIPFFGPGIEGLYTAGLIKNQNLVCLRLRLAN QTAQSLELLRVTTEERTFSLNRHAIDFLLARWGGTCKVLDGPD CIGIEDLSRNISEQIDQIKKDEKQEGTWGLGGKWWTSDWGV LTNLGILLLSIAVLIALSCICRIFTKYIG

**GP immunogen sequences for MARV expansion vaccines**

*Marburg marburgvirus*—Ravn cluster consensus (MARV-RAVV CON VACCINE); (Ravn, Durba (09DRC99) and Uganda (02Uga07)): MKTIYFLI SLILIQSIKTLPLVLEIASNSQPQDVDSVCSGTLQKTEDVHLMGFTLS GQKVADSPLEASKRWAFTGVPKNEVEYTEGEEAKTCYNISVTDPSGK SLLDPPSNIRDYPKCKTVHHIQGNPHAQGIALHLWGAFFLYDRVAST MYRGKVFTEGNIAAMIVNKTVHRMIFSRQGGQYRHMNLTSTNKY WTSSNETRRNDTGCFCGILQEYNSTNNQTCPSLKPPLPTVTPSIHSTNTQ INTAKSGTMMNPSSDDEDLMSISGSGEQQPHTTLNVVTEQKQSSTIL STPSLHSTSQHEQNSTPSRHAVTEHNGTDPTTQPATLLNNTNTTP TYNTLKYNLSTPSPTRNITNNDTQRELAESEQTNAQLNNTLDPTENPT TAQDTNSTNIIMTSDITSKHPTNSSPDSPTTRPIYFRKKRSIFWKEG DIFPFLDGLINTEIDFDPINTEIFDESFSNTSTNEEQHTPPNISLTFSYF PDKNGDTAYSGENENDCDAELRIWSVQEDDLAAGLSWIPFFPGIEGLY TAGLIKNNLVCLRLRLANQTAKSLELLLRVTTEERTFSLINRHAIIDFL TRWGGTCKVLGPDCCIGIEDLSKNISEQIDKIRKDEQKEETGWGLGGKW WTSWGWVLTNLGILLLSIAVLIALSCICRIFTKYIG

*Marburg marburgvirus*—Ozolin cluster consensus (MARV-OZO CON VACCINE); (Ozolin, Uganda (01Uga07), and Durba (05 and 07DRC99)): MRTTCFFISLILIQGIKTLPILEIASNDQPQNVDSVCSGTLQKTED VHLMGFTLSGQKVADSPLEASKRWAFTGVPKNEVEYTEGEE AKTCYNISVTDPSGKSLLDPPNTNRDYPKCKTIHHIQGNPHAQ GIALHLWGAFFLYDRIASTMYRGKVFTEGNIAAMIVNKTVHK MIFSRQGGQYRHMNLTSTNKYWTSSNGTQNTDTCFCGTLQEYN STKNQTCAPSKTPPPPTARPEIKPTSTPTDATRLNNTNPNSD DEDLTTSGSGSGEQEPYTTSDAVTKQLSSTMPPTPSPQPGTPQQG GNNTNHSQDAATELDNTNTTAQPPTPSHNTTITSTNNTSKHNL STLSEPPQNTTNPNTQSMATENEKTSAPPKTTLPPTESPTTEK STNNTKSPPTMEPNTTNGHFTSPSSTPNSTTQHLYFRKRKRSIL WREGDMFPFLDGLINAPIDFDPVNTKTFDESSSGASAEEDQHAS SNISLTLSPHTSENTAYSGENENDCDAELRIWSVQEDDLAAGLS WIPFFPGIEGLYTAGLIKNNLVCLRLRLANQTAKSLELLLRVT TEERTFSLINRHAIIDFLTRWGGTCKVLGPDCCIGIEDLSRNISEQ IDQIKKDEQKEGTGWGLGGKWWTSWGWVLTNLGILLLSIAV LIALSCICRIFTKYIG

*Marburg marburgvirus*—Musoke cluster consensus (MARV-MUS CON VACCINE); (Musoke, Popp, and Leiden): MKTTCLFISLILIQGIK TLPPILEIASNNQPQNVDSVCSGTLQKTEDVHLMGFTLSGQKVAD SPLEASKRWAFTGVPKNEVEYTEGEEAKTCYNISVTDPSGKSLLD DPPTNIRDYPKCKTIHHIQGNPHAQGIALHLWGAFFLYDRI ASTMYRGRVTEGNIAAMIVNKTVHKMIFSRQGGQYRHMNLT STNKYWTSSNGTQNTDTCFCGALQEYNSTKNQTCAPSKIPSPLP TARPEIKPTSTPTDATKLNNTDPNSDDEDLATSGSGSGEQEPHTTS DAVTKQLSSTMPPTPSPQSPTPQEGNNTDHSQDAVTEPNKNTNT TAQPSMPPHNTTAISTNNTSKHNFSTLSAPLQNTTNYDTQSTATEN EQTSAPSKTTLPTGNLTTAKSTNNTKGPPTTAPNMTNGHLSPT SPTPNPTTQHLVYFRKKRSILWREGDMFPFLDGLINAPIDFD PVPNTKTFDESSSGASAEEDQHASPNSLTLSPNINENTAY SGENENDCDAELRIWSVQEDDLAAGLSWIPFFPGIEGLYTA GLIKNNLVCLRLRLANQTAKSLELLLRVTTEERTFSLINRHAIID FLTRWGGTCKVLGPDCCIGIEDLSRNISEQIDQIKKDEQKEGTGW GLGGKWWTSWGWVLTNLGILLLSIAVLIALSCICRIFTKYIG

**Transfections and immunoblotting.** Human Embryonic Kidney (HEK) 293T cells were cultured, transfected, and harvested as described previously.<sup>45</sup> Briefly, cells were grown in DMEM with 10% fetal bovine serum (FBS), 1% Pen-strep, sodium pyruvate, and L-glutamine. Cells were cultured in 150 mm Corning dishes and grown to 70% confluence overnight in a 37° incubator with 5% CO<sub>2</sub>. Dishes were transfected with 10–25 µg of *Filoviridae* pDNA using either a Calphos Mammalian Transfection Kit protocol (Clontech) or Lipofectamine 2000 reagent (Invitrogen) per the manufacturer's protocol and then incubated for 24–48 hours. Cells were harvested with ice cold phosphate-buffered saline (PBS), centrifuged and washed, and then pelleted for Western immunoblot or FACS analysis.

Standard western blotting was used and GP-specific MAbs for GP1 detection were generated as described.<sup>46</sup>

**Animals, vaccinations, and challenge.** Adult female C57BL/6 (H-2<sup>b</sup>), BALB/cj (H-2<sup>d</sup>), and B10.Br (H-2<sup>k</sup>) mice were purchased from The Jackson Laboratory (Bar Harbor, ME), whereas Hartley guinea pigs were from Charles River (Wilmington, MA). All animal experimentation was conducted following UPenn IACUC and School of Medicine Animal Facility, or NML Institutional Animal Care Committee of the PHAC and the Canadian Council on Animal Care guidelines for housing and care of laboratory animals and performed in accordance with recommendations in the Guide for the Care and Use of Laboratory Animals of NIH after pertinent review and approval by the abovementioned institutions. UPenn and NML comply with NIH policy on animal welfare, the Animal Welfare Act, and all other applicable federal, state, and local laws.

Mice were immunized i.m. by needle injection with 40 µg of plasmid resuspended in water, whereas guinea pigs were immunized i.d., with 200 µg of each into three separate vaccination sites. Vaccinations were immediately followed by electroporation at the same site as previously described.<sup>45</sup> Briefly, a three-pronged CELLECTRA adaptive constant current Minimally Invasive Device was inserted ~2 mm i.d. (Inovio Pharmaceuticals, Blue Bell, PA). Square-wave pulses were delivered through a triangular 3-electrode array consisting of 26-gauge solid stainless steel electrodes and two constant current pulses of 0.1 Amps were delivered for 52 microsecond/pulse separated by a 1 second delay.

For lethal challenge studies, challenges were limited to rodent-adapted ZEBOV and MARV, as SUDV adapted for lethality in rodents are not yet available. Guinea pigs were challenged 28 days after the final vaccination by i.p. injection with 1,000 LD<sub>50</sub> of guinea pig-adapted ZEBOV (21.3 FFU/animal)<sup>47</sup> or 1,000 LD<sub>50</sub> MARV-Angola (681 TCID<sub>50</sub>/animal), which was made in-house. Briefly, the guinea pig-adapted MARV was made by the serial passage of wild-type MARV-Angola in outbred adult female Hartley guinea pigs. Seven days after inoculation, the animals were euthanized and livers were harvested and homogenized. This homogenate was then injected i.p. into naïve adult guinea pigs and the process repeated until animals lost weight, gloss of hair, and succumbed to infection similar to EBOV adaptation in guinea pigs. For mouse lethal challenge studies,<sup>30</sup> mice were injected i.p. with 200 µl of a 1,000 LD<sub>50</sub> (10 FFU/animal) of mouse-adapted ZEBOV. All animals were weighed daily and monitored for disease progression using an approved score sheet for at least 18 days for mice and 22 days for guinea pigs. All infectious work was performed in a "Biosafety Level 4" (BSL-4) facility at NML, PHAC.

**ELISA and neutralization assays.** Ab titers were determined using 96-well ELISA plates coated with either sucrose-purified MARV-Ozolin GP or ZGP (SGP was not available for this study), or with negative control sucrose-purified Nipah G protein at a concentration of 1:2,000, as previously described.<sup>46</sup> Briefly, the plates were then incubated for 18 hours at 4 °C, washed with PBS and 0.1% Tween-20, and 100 µl/sample of the sera were tested in triplicate (at dilutions 1:100, 1:400, 1:1,600, and 1:6,400 in PBS with 5% skim milk and 0.5% Tween-20). Following an incubation at 37 °C for 1 hour in a moist container, the plates were washed and then 100 µl of goat antimouse IgG-conjugated HRP antibody (Cedarlane, Burlington, NC) was added (1:2,000 dilution) and incubated for another 37 °C for 1 hour in a moist container. After a wash, 100 µl of the ABST (2,2'-azino-bis(3-ethylbenzothiazoline-6-sulphonic acid) and peroxidase substrate (Cedarlane) was added to visualize Ab binding. Again in a moist container, the plate was incubated for 30 minutes at 37 °C and then later read at 405 nm. Positive binding results were characterized by being >3 SD when subtracting the positive control from the negative control serum.

The ZEBOV neutralization assay was performed as previously described.<sup>39</sup> Briefly, Sera collected from immunized mice and guinea pigs were inactivated at 56°C for 45 minutes and serial dilutions of each sample (1:20, 1:40, etc., for mice and 1:50 for guinea pigs, in 50 µl of

DMEM) was mixed with equal volume of ZEBOV expressing the enhanced green fluorescent protein (EGFP) reporter gene (ZEBOV-EGFP) (100 transducing units/well, according to EGFP expression) and incubated at 37 °C for 90 minutes. The mixture was then transferred onto subconfluent VeroE6 cells in 96-well flat-bottomed plates and incubated for 5–10 minutes at room temperature. Control wells were infected with equal amounts of the ZEBOV-EGFP virus without addition of serum or with non-immune serum. DMEM of 100  $\mu$ l supplemented with 20% FBS was then added to each well, and plates were incubated at 37 °C in 5% CO<sub>2</sub> for 48 hours. Alternatively, neutralization of MARV-Angola 368 was assessed using an immunofluorescent assay. A primary rabbit anti-MARV Ab and secondary goat antirabbit IgG FITC-conjugated Ab was used for detection. NABs against SUDV-Boniface were assayed based on cytopathic effect on CV-1 cells. Cells were incubated with equal parts of immunized sera and SUDV-Boniface for 10 days before subsequently fixed with 10% buffered formalin for 24 hours and examined under a light microscope. EGFP and FITC positive cells were counted in each well and sample dilutions showing >50% reduction in the number of green cells compared with controls scored positive for NAB. Alternatively, NABs against SUDV-Boniface were assayed based on cytopathic effect on CV-1 cells. All infectious work was performed in the BSL-4 laboratory of NML, PHAC.

**Splenocyte isolation.** Spleens were harvested 8–11 days following the final immunization as previously described.<sup>45</sup> Briefly, spleens were placed in RPMI 1640 medium (Mediatech, Manassas, VA) supplemented with 10% FBS, 1X Antibiotic-Antimycotic (Invitrogen), and 1X  $\beta$ -ME (Invitrogen). Splenocytes were isolated by mechanical disruption of the spleen using a Stomacher machine (Seward Laboratory Systems, Bohemia, NY), and the resulting product was filtered using a 40  $\mu$ m cell strainer (BD Biosciences, San Jose, CA). The cells were then treated for 5 minutes with ACK lysis buffer (Lonza, Switzerland) for lysis of RBCs, washed in PBS, and then resuspended in RPMI medium for use in ELISPOT or FACS assay.

**ELISPOT assays.** Standard IFN $\gamma$  ELISPOT assay has been described.<sup>45</sup> Briefly, 96-well plates (Millipore, Billerica, MA) were coated with antimouse IFN capture antibody and incubated for 24 hours at 4 °C (R&D Systems, Minneapolis, MN). The following day, plates were washed with PBS and then blocked for 2 hours with blocking buffer (1% BSA and 5% sucrose in PBS). Splenocytes (1–2  $\times$  10<sup>5</sup> cells/well) were plated in triplicate and stimulated overnight at 37°C in 5% CO<sub>2</sub> and in the presence of either RPMI 1640 (negative control), Con A (positive control), or GP peptides either individually (15-mers overlapping by 9 amino acids and spanning the lengths of their respective GP) or whole pooled (2.5  $\mu$ g/ml final). After 18–24 hours of stimulation, the plates were washed in PBS and then incubated for 24 hours at 4 °C with biotinylated antimouse IFN $\gamma$ Ab (R&D Systems). Next, the plates were washed again in PBS, and streptavidin-alkaline phosphatase (MabTech, Nacka Strand, Sweden) was added to each well and incubated for 2 hours at room temperature. Lastly, the plates were washed again in PBS and then BCIP/NBT Plus substrate (MabTech) was added to each well for 5–30 minutes for spot development. As soon as the development process was complete upon visual inspection, the plate was rinsed with distilled water and then dried overnight at room temperature. Spots were enumerated using an automated ELISPOT reader (Cellular Technology, Shaker Heights, OH).

For comprehensive analysis of T-cell breadth, standard IFN $\gamma$  ELISPOT was modified herein as previously described.<sup>21</sup> Identification and measurement of subdominant and immunodominant T-cell epitopes were assessed by stimulating splenocytes with individual peptides as opposed to whole or matrix peptide pools; the traditional practice of pooling peptides for the sake of sample preservation, such as the use of matrix array pools, results in a reduction of assay sensitivity, because total functional responses in pools containing multiple epitope-displaying peptides will effectively lower assay resolution, *i.e.*, “drown-out” those of lower magnitude. Thus, modified ELISPOT was performed with individual peptides (15-mers overlapping

by 9 amino acids; 2.5  $\mu$ g/ml final) spanning each GP immunogen. Peptides containing T-cell epitopes were identified ( $\geq$ 10 average IFN $\gamma$ <sup>+</sup> spots and  $\geq$ 80% animal response rate; summarized in **Table 1**) and then later confirmed functionally and phenotypically by FACS. No shared or partial epitopes were identified (data not shown), nor did FACS data or web-based epitope prediction software (www.iedb.org; **Table 1**) suggest the presence of a CD4<sup>+</sup> or CD8<sup>+</sup> T-cell epitope that was preserved within consecutive peptides. Here, possible shared/partial T-cell epitopes were addressed for all instances of contiguous peptide responses as identified by modified ELISPOT assay. Cells were stimulated individually with each of the contiguous peptides, as well as paired in combination for direct comparison, and were defined as “shared/partial” if the combined response was not greater than either of the two individual responses. Also, it must be noted, that the epitopic response presented herein may not have been completely comprehensive, because the “15-mer overlapping by 9 amino acids” algorithm for generating peptides is biased towards complete coverage of CD8 T-cell epitopes which may underestimate CD4 T-cell responses due to the nature of class II-restricted epitopes being longer than 15 amino acids. Lastly, amino acid similarity plots were generated using Vector NTI software (**Figure 4b**).

**Flow cytometry.** Splenocytes were added to a 96-well plate (1  $\times$  10<sup>6</sup> cells/well) and stimulated for 5–6 hours with either individual peptides or “Minimal Peptide Pools” (2.5  $\mu$ g/ml final). Individual peptides stimulation was used for functional confirmation of all peptides identified by modified ELISPOT (**Table 1**) as well as phenotypic characterization. Splenocytes and transfected 293Ts were first prestained with LIVE/DEAD Fixable Violet Dead Cell Stain Kit (Invitrogen). For splenocytes, cells were surface-stained for CD19 (V450; clone 1D3), CD4 (PE-Cy7; clone RM4-5), CD8 (APC-Cy7; clone 53–6.7), and CD44 (PE-Cy5; clone IM7) (BD Biosciences), washed three times in PBS + 1% FBS, permeabilized with BD Cytofix/Cytoperm kit, and then stained intracellularly with IFN $\gamma$  (APC; clone XMG1.2), TNF (FITC; clone MP6-XT22), CD3 (PE-cy5.5; clone 145-2C11), and T-bet (PE; clone 4B10) (eBioscience). GP expression in transfected 293T cells was assessed 24 hours after transfection. Indirect staining was performed following a 30 minutes incubation at 4 °C in PBS + 1% FBS containing the indicated mouse-derived GP-specific polyclonal serum reagent (1:200 dilution), each produced by pooling serum from H-2<sup>b</sup> mice immunized three times with their respective E-DNA vaccine or pVAX1 empty vector control. Cells were then stained with FITC-conjugated goat antimouse IgG (BioLegend, San Diego, CA), washed extensively, and then stained for MHC class I (HLA-ABC; PE-Cy7; clone G46-2.6; BD Biosciences). All cells were fixed in 1% paraformaldehyde. All data were collected using a LSRII flow cytometer (BD Biosciences) and analyzed using FlowJo software (Tree Star, Ashland, OR). Splenocytes were gated for activated IFN $\gamma$ -producing T cells that were CD3<sup>+</sup> CD44<sup>+</sup>, CD4<sup>+</sup>, or CD8<sup>+</sup>, and negative for the B cell marker CD19 and viability dye (see **Supplementary Figure S1**).

**Statistical analysis.** Significance for unrooted phylogenetic trees was determined by maximum-likelihood method and verified by bootstrap analysis and significant support values ( $\geq$ 80%; 1,000 bootstrap replicates) were determined by MEGA version 5 software. Group analyses were completed by matched, two-tailed, unpaired *t*-test and survival curves were analyzed by log-rank (Mantel-Cox) test. All values are mean  $\pm$  SEM and statistical analyses were performed by GraphPad Prism (La Jolla, CA).

## SUPPLEMENTARY MATERIAL

**Figure S1.** GP-specific T-cell-gating strategy.

**Figure S2.** Vaccination generated robust T cells.

**Figure S3.** T-cell induction by “single-dose” vaccination.

**Note S1.** Vaccine-induced immunity contributes to protection in pre-clinical studies.

**Note S2.** Diversity among the *Filoviridae* is relatively high.

**Note S3.** Enhanced DNA vaccination.

**Note S4.** Rodent preclinical models.

## ACKNOWLEDGMENTS

We acknowledge Karuppihan Muthumani, and members of the Weiner and Kobinger laboratories for significant discussion, contributions, and/or critical reading of this manuscript. In addition, Charles H Pletcher, Andrew D Bantly, Richard D Schretzenmair, William J DeMuth III, Gisela N BrakeSillá, and the University of Pennsylvania Path BioResource Flow Cytometry & Cell Sorting Facility staff are acknowledged for their generous technical assistance. This work was supported by NIH, NIAID, and/or DAIDS grants: HIV Vaccine Research and Design (HIVRAD) (P01-AI071739) and "Development of a Universal Influenza Seasonal Vaccine" (R01-AI092843) to D.B.W., and by funding to D.B.W. and D.J.S. (T32-AI070099). Also, the work was supported in part by "Evaluation of Protective Immunity after Mucosal Vaccination Against Ebola Virus" (V01-AI078045). In addition, funding from Inovio Pharmaceuticals was received as part of Sponsored Research Agreements entitled "Study and Development of Consensus Immunogens in the area of Viral Vaccines" and "Consensus Immunogens." For disclosure purposes, D.B.W. notes that he and his laboratory have several commercial relationships with companies in the area of vaccines. These include him receiving consulting fees or stock ownership for Advisory/Review Board service, speaking support, or research support from commercial entities including Inovio Pharmaceuticals, Bristol-Myers Squibb, VGXI, Pfizer, Virxsys Co., Johnson & Johnson, Merck & Co., Sanofi Pasteur, Althea, Novo Nordisk, Statens Serum Institut, Aldevron, Novartis, Incyte, and possibly others. The other authors declare no conflict of interest.

## REFERENCES

- Feldmann, H and Geisbert, TW (2011). Ebola haemorrhagic fever. *Lancet* **377**: 849–862.
- MacNeil, A and Rollin, PE (2012). Ebola and Marburg hemorrhagic fevers: neglected tropical diseases? *PLoS Negl Trop Dis* **6**: e1546.
- Borio, L, Inglesby, T, Peters, CJ, Schmaljohn, AL, Hughes, JM, Jahrling, PB *et al.*; Working Group on Civilian Biodefense. (2002). Hemorrhagic fever viruses as biological weapons: medical and public health management. *JAMA* **287**: 2391–2405.
- Warfield, KL and Olinger, GG (2011). Protective role of cytotoxic T lymphocytes in filovirus hemorrhagic fever. *J Biomed Biotechnol* **2011**: 984241.
- Wauquier, N, Becquart, P, Padilla, C, Baize, S and Leroy, EM (2010). Human fatal zaire ebola virus infection is associated with an aberrant innate immunity and with massive lymphocyte apoptosis. *PLoS Negl Trop Dis* **4**: e837.
- Falzarano, D, Geisbert, TW and Feldmann, H (2011). Progress in filovirus vaccine development: evaluating the potential for clinical use. *Expert Rev Vaccines* **10**: 63–77.
- Warfield, KL, Olinger, G, Deal, EM, Swenson, DL, Bailey, M, Negley, DL *et al.* (2005). Induction of humoral and CD8+ T cell responses are required for protection against lethal Ebola virus infection. *J Immunol* **175**: 1184–1191.
- Grant-Klein, RJ, Altamura, LA and Schmaljohn, CS (2011). Progress in recombinant DNA-derived vaccines for Lassa virus and filoviruses. *Virus Res* **162**: 148–161.
- Kalina, WV, Warfield, KL, Olinger, GG and Bavari, S (2009). Discovery of common marburgvirus protective epitopes in a BALB/c mouse model. *Virology* **393**: 132.
- Olinger, GG, Bailey, MA, Dye, JM, Bakken, R, Kuehne, A, Kondig, J *et al.* (2005). Protective cytotoxic T-cell responses induced by venezuelan equine encephalitis virus replicons expressing Ebola virus proteins. *J Virol* **79**: 14189–14196.
- Sullivan, NJ, Hensley, L, Asiedu, C, Geisbert, TW, Stanley, D, Johnson, J *et al.* (2011). CD8+ cellular immunity mediates rAd5 vaccine protection against Ebola virus infection of nonhuman primates. *Nat Med* **17**: 1128–1131.
- Geisbert, TW, Bailey, M, Geisbert, JB, Asiedu, C, Roederer, M, Grazia-Pau, M *et al.* (2010). Vector choice determines immunogenicity and potency of genetic vaccines against Angola Marburg virus in nonhuman primates. *J Virol* **84**: 10386–10394.
- Fenimore, PW, Muhammad, MA, Fischer, WM, Foley, BT, Bakken, RR, Thurmond, JR *et al.* (2012). Designing and testing broadly-protective filoviral vaccines optimized for cytotoxic T-lymphocyte epitope coverage. *PLoS ONE* **7**: e44769.
- Hensley, LE, Mulangu, S, Asiedu, C, Johnson, J, Honko, AN, Stanley, D *et al.* (2010). Demonstration of cross-protective vaccine immunity against an emerging pathogenic Ebolavirus Species. *PLoS Pathog* **6**: e1000904.
- Zahn, R, Gillisen, G, Roos, A, Koning, M, van der Helm, E, Spek, D *et al.* (2012). Ad35 and ad26 vaccine vectors induce potent and cross-reactive antibody and T-cell responses to multiple filovirus species. *PLoS ONE* **7**: e44115.
- Geisbert, TW and Feldmann, H (2011). Recombinant vesicular stomatitis virus-based vaccines against Ebola and Marburg virus infections. *J Infect Dis* **204** Suppl 3: S1075–S1081.
- Grant-Klein, RJ, Van Deusen, NM, Badger, CV, Hannaman, D, Dupuy, LC and Schmaljohn, CS (2012). A multiagent filovirus DNA vaccine delivered by intramuscular electroporation completely protects mice from ebola and Marburg virus challenge. *Hum Vaccin Immunother* **8**: 1703–1706.
- Bagarazzi, ML, Yan, J, Morrow, MP, Shen, X, Parker, RL, Lee, JC *et al.* (2012). Immunotherapy against HPV16/18 generates potent TH1 and cytotoxic cellular immune responses. *Sci Transl Med* **4**: 155ra138.
- Kee, ST, Gehl, J, Lee, EW (2011). *Clinical Aspects of Electroporation*. Springer: New York, NY.
- Hirao, LA, Draghia-Akli, R, Prigge, JT, Yang, M, Sathishchandran, A, Wu, L *et al.* (2011). Multivalent smallpox DNA vaccine delivered by intradermal electroporation drives protective immunity in nonhuman primates against lethal monkeypox challenge. *J Infect Dis* **203**: 95–102.
- Shedlock, DJ, Talbott, KT, Wu, SJ, Wilson, CM, Muthumani, K, Boyer, JD *et al.* (2012). Vaccination with synthetic constructs expressing cytomegalovirus immunogens is highly T cell immunogenic in mice. *Hum Vaccin Immunother* **8**: 1668–1681.
- Towner, JS, Khristova, ML, Sealy, TK, Vincent, MJ, Erickson, BR, Bawiec, DA *et al.* (2006). Marburgvirus genomics and association with a large hemorrhagic fever outbreak in Angola. *J Virol* **80**: 6497–6516.
- Francica, JR, Varela-Rohena, A, Medvec, A, Plesa, G, Riley, JL and Bates, P (2010). Steric shielding of surface epitopes and impaired immune recognition induced by the ebola virus glycoprotein. *PLoS Pathog* **6**: e1001098.
- Hersperger, AR, Martin, JN, Shin, LY, Sheth, PM, Kovacs, CM, Cosma, GL *et al.* (2011). Increased HIV-specific CD8+ T-cell cytotoxic potential in HIV elite controllers is associated with T-bet expression. *Blood* **117**: 3799–3808.
- Sullivan, NJ, Sanchez, A, Rollin, PE, Yang, ZY and Nabel, GJ (2000). Development of a preventive vaccine for Ebola virus infection in primates. *Nature* **408**: 605–609.
- Dowling, W, Thompson, E, Badger, C, Mellquist, JL, Garrison, AR, Smith, JM *et al.* (2007). Influences of glycosylation on antigenicity, immunogenicity, and protective efficacy of ebola virus GP DNA vaccines. *J Virol* **81**: 1821–1837.
- Vanderzanden, L, Bray, M, Fuller, D, Roberts, T, Custer, D, Spik, K *et al.* (1998). DNA vaccines expressing either the GP or NP genes of Ebola virus protect mice from lethal challenge. *Virology* **246**: 134–144.
- Riemschneider, J, Garrison, A, Geisbert, J, Jahrling, P, Hevey, M, Negley, D *et al.* (2003). Comparison of individual and combination DNA vaccines for B. anthracis, Ebola virus, Marburg virus and Venezuelan equine encephalitis virus. *Vaccine* **21**: 4071–4080.
- Swenson, DL, Warfield, KL, Negley, DL, Schmaljohn, A, Aman, MJ and Bavari, S (2005). Virus-like particles exhibit potential as a pan-filovirus vaccine for both Ebola and Marburg viral infections. *Vaccine* **23**: 3033–3042.
- Kobinger, GP, Feldmann, H, Zhi, Y, Schumer, G, Gao, G, Feldmann, F *et al.* (2006). Chimpanzee adenovirus vaccine protects against Zaire Ebola virus. *Virology* **346**: 394–401.
- Jones, SM, Stroher, U, Fernando, L, Qiu, X, Alimonti, J, Melito, P *et al.* (2007). Assessment of a vesicular stomatitis virus-based vaccine by use of the mouse model of Ebola virus hemorrhagic fever. *J Infect Dis* **196** Suppl 2: S404–S412.
- Dowling, W, Thompson, E, Badger, C, Mellquist, JL, Garrison, AR, Smith, JM *et al.* (2007). Influences of glycosylation on antigenicity, immunogenicity, and protective efficacy of ebola virus GP DNA vaccines. *J Virol* **81**: 1821–1837.
- Shedlock, DJ, Bailey, MA, Popernack, PM, Cunningham, JM, Burton, DR and Sullivan, NJ (2010). Antibody-mediated neutralization of Ebola virus can occur by two distinct mechanisms. *Virology* **401**: 228–235.
- Sullivan, NJ, Geisbert, TW, Geisbert, JB, Shedlock, DJ, Xu, L, Lamoreaux, L *et al.* (2006). Immune protection of nonhuman primates against Ebola virus with single low-dose adenovirus vectors encoding modified GPs. *PLoS Med* **3**: e177.
- Xu, L, Sanchez, A, Yang, Z, Zaki, SR, Nabel, EG, Nichol, ST *et al.* (1998). Immunization for Ebola virus infection. *Nat Med* **4**: 37–42.
- Warfield, KL, Swenson, DL, Olinger, GG, Kalina, WV, Aman, MJ and Bavari, S (2007). Ebola virus-like particle-based vaccine protects nonhuman primates against lethal Ebola virus challenge. *J Infect Dis* **196** Suppl 2: S430–S437.
- Sun, Y, Carrion, R Jr, Ye, L, Wen, Z, Ro, YT, Brasky, K *et al.* (2009). Protection against lethal challenge by Ebola virus-like particles produced in insect cells. *Virology* **383**: 12–21.
- Choi, JH, Schafer, SC, Zhang, L, Kobinger, GP, Juelich, T, Freiberg, AN *et al.* (2012). A single sublingual dose of an adenovirus-based vaccine protects against lethal Ebola challenge in mice and guinea pigs. *Mol Pharm* **9**: 156–167.
- Richardson, JS, Yao, MK, Tran, KN, Croyle, MA, Strong, JE, Feldmann, H *et al.* (2009). Enhanced protection against Ebola virus mediated by an improved adenovirus-based vaccine. *PLoS ONE* **4**: e5308.
- Blaney, JE, Wirblich, C, Papaneri, AB, Johnson, RF, Myers, CJ, Juelich, TL *et al.* (2011). Inactivated or live-attenuated bivalent vaccines that confer protection against rabies and Ebola viruses. *J Virol* **85**: 10605–10616.
- Ebert, S, Lemmermann, NA, Thomas, D, Renzaho, A, Reddehase, MJ and Holtappels, R (2012). Immune control in the absence of immunodominant epitopes: implications for immunotherapy of cytomegalovirus infection with antiviral CD8+ T cells. *Med Microbiol Immunol* **201**: 541–550.
- Ruckwardt, TJ, Luongo, C, Malloy, AM, Liu, J, Chen, M, Collins, PL *et al.* (2010). Responses against a subdominant CD8+ T cell epitope protect against immunopathology caused by a dominant epitope. *J Immunol* **185**: 4673–4680.
- Laddy, DJ, Yan, J, Kutzler, M, Kobasa, D, Kobinger, GP, Khan, AS *et al.* (2008). Heterosubtypic protection against pathogenic human and avian influenza viruses via *in vivo* electroporation of synthetic consensus DNA antigens. *PLoS ONE* **3**: e2517.
- Yan, J, Yoon, H, Kumar, S, Ramanathan, MP, Corbitt, N, Kutzler, M *et al.* (2007). Enhanced cellular immune responses elicited by an engineered HIV-1 subtype B consensus-based envelope DNA vaccine. *Mol Ther* **15**: 411–421.
- Shedlock, DJ, Talbott, KT, Wu, SJ, Wilson, CM, Muthumani, K, Boyer, JD *et al.* (2012). Vaccination with synthetic constructs expressing cytomegalovirus immunogens is highly T cell immunogenic in mice. *Hum Vaccin Immunother* **8**: 1668–1681.
- Qiu, X, Alimonti, JB, Melito, PL, Fernando, L, Stroher, U and Jones, SM (2011). Characterization of Zaire ebolavirus glycoprotein-specific monoclonal antibodies. *Clin Immunol* **141**: 218–227.
- Richardson, JS, Abou, MC, Tran, KN, Kumar, A, Sahai, BM and Kobinger, GP (2011). Impact of systemic or mucosal immunity to adenovirus on Ad-based Ebola virus vaccine efficacy in guinea pigs. *J Infect Dis* **204** Suppl 3: S1032–S1042.
- Warfield, KL, Posten, NA, Swenson, DL, Olinger, GG, Esposito, D, Gillette, WK *et al.* (2007). Filovirus-like particles produced in insect cells: immunogenicity and protection in rodents. *J Infect Dis* **196** Suppl 2: S421–S429.
- Rao, M, Bray, M, Alving, CR, Jahrling, P and Matyas, GR (2002). Induction of immune responses in mice and monkeys to Ebola virus after immunization with liposome-encapsulated irradiated Ebola virus: protection in mice requires CD4(+) T cells. *J Virol* **76**: 9176–9185.
- Rao, M, Matyas, GR, Grieder, F, Anderson, K, Jahrling, PB and Alving, CR (1999). Cytotoxic T lymphocytes to Ebola Zaire virus are induced in mice by immunization with liposomes containing lipid A. *Vaccine* **17**: 2991–2998.